Pergamon

0013-7944(94)E0031-B

Engineering Fracture Mechanics Vol. 48, No. 5, pp. 629–640, 1994

0013-7944/94 $7.00 + 0.00

CONTINUUM MODEL OF THE STRUCTURAL-INHOMOGENEOUS POROUS BODY AND ITS APPLICATION FOR THE STUDY OF STABILITY AND VISCOUS FRACTURE OF MATERIALS DEFORMED UNDER PRESSURE

JA. E. BEIGELZIMER, B. M. EFROS, V. N. VARYUKHIN and A. V. KHOKHLOV

Donetsk Physico-Technical Institute of the Ukrainian Academy of Sciences, R. Luxemburg str., 72, Donetsk 340114, Ukraine

Abstract—A mathematical model of plastic deformation of structurally inhomogeneous material with defects of inhomogeneity-type has been developed. Principal relationships have been obtained which are based on the results of physical investigations. The proposed model has been used as a basis for the investigation of viscous fracture and deformation localization in pressure treatment of compact and noncompact materials. The model has been compared with experiment both qualitatively and quantitatively.

1. INTRODUCTION

It is well known (see e.g. ref. [1]) that the plastic deformation of solids is accompanied by microfractures, i.e. by appearance and accumulation of microinhomogeneities. The latter result in loosening of material and finally may give rise to localization of deformation and macroscopic fracture. The intensity of microfracture is substantially affected by the magnitude of the hydrostatic component of the stress tensor. It was shown [2, 3] that the increase in hydrostatic pressure allows one to achieve large magnitudes of deformation before fracture and to raise the resistance of the material against the deformation localization. This effect is used in practice, in particular in hydrostatic treatment of materials [4, 5].

The development of the hydrostatic treatment technologies should be based on the mathematical models describing microfracture of solids at deformation and taking into account the pressure effect on this process.

An adequate description of the microfracture is possible in the framework of the continuum concepts. In this case the consideration involves the magnitude of porosity which is the total relative volume of microdefects. Thus the task is reduced to obtaining the kinetic equation for this value [6].

The application of the flow theory apparatus allows one to obtain the kinetic equation for porosity on the basis of the assumption of dependence of the loading function on the hydrostatic component of the stress tensor.

In the literature there are two groups of the physically grounded loading functions satisfying this assumption. The first corresponds to the condition of the ultimate equilibrium of bulk materials [7], and the second corresponds to the porous body plasticity conditions [6].

The models [7] based on the first group of loading functions do not allow one to take into account the pressure effect on the intensity of the microdefect nucleation. Moreover, they do not describe healing of microdefects under pressure.

The models of the second group take into account the possibility of microscopic healing. However, to describe the loosening of a solid body at deformation the authors of refs [8, 9] had to make an additional assumption going beyond the flow theory framework. It is connected with the introduction of the terms describing the formation of micropores into the kinetic equation for porosity directly omitting the loading function. This is equivalent to giving up the gradient condition.

It is well known that this condition has no thermodynamic grounding and can be ignored. Nevertheless, numerous papers based on this condition give evidence that in lots of cases it is in rather good agreement with experiment. Therefore, we believe it to be interesting to describe the

microfracture process without giving up the gradient condition by taking into account all the main effects in the expression for the loading function. It is this attempt that is made in this paper.

2. PHYSICAL PRECONDITIONS OF THE DEFORMABLE SOLID MODEL

While constructing the physical model of a structurally inhomogeneous solid deformed under pressure we shall be guided by the results of the physical studies presented in refs [1, 10].

First of all let us note that in view of structural inhomogeneity of the material its plastic deformation as a whole can be realized only by means of joint coordinated deformation of its structural elements. The latter, however, cannot, as a rule, deform in an arbitrary way (i.e. fewer than five slip systems work). Therefore, as the material is loaded breaking of microshifts takes place giving rise to internal microstresses. The latter are the main cause of the strain-hardening at relatively small plastic deformations.

Microstresses cannot grow infinitely. At a certain level they relax either due to formation of elementary micropores or to inclusion of new channels of plastic accommodation. The latter, as a rule, are associated with the splitting of structural elements into smaller ones and their turning around with respect to each other. The fact that the structural elements become smaller results in growth of the forces of the internal friction-type and that is the principal mechanism of hardening at large plastic deformation.

The above picture of the plastic deformation evolution allowed a number of authors [7, 11] to put forward a physical model of a solid as a bulk medium whose elements are interconnected by means of thin glueing interlayers which are highly resistant to tearing-off and weakly resistant to shear. In the course of deformation there is relative shift and rotation of the medium elements.

On the basis of this model the authors of ref. [7] proposed the principal relationships for description of the material loosening at deformation.

We can improve this model to extend it to the physical investigations of the hydrostatic pressure effect on the plastic deformation mechanisms [10]. Let us assume that the structural elements of the bulk medium cannot only shift and rotate but may also split and plastically deform, thus adjusting themselves to each other. The ability to be accommodated is determined by the plastic deformation mechanisms acting at this or that moment. If they provide arbitrary deformation of the structural elements (e.g. five slip systems work), complete accommodation is possible. Otherwise accommodation is only partial. As a result, gaps (or microinhomogeneities) appear between the elements (if at the beginning the elements were closely adjusted to each other), which results in loosening of the material.

If, on the other hand, the microinhomogeneities were present before the deformation, they may disappear at certain conditions since the structural elements are able to adjust to each other.

Thus the proposed material can demonstrate both appearance and healing of microinhomogeneities which makes it different from the conventional models of a porous body [6, 12] where the body carcass (matrix) is supposed to have no structure of its own and to deform as a continuum. The latter corresponds to the limiting case where the structural elements in the above model of a solid body can adapt to each other completely at joint plastic deformation.

Let us introduce some measure of restrictions to the joint plastic deformation of separate structural elements and characterise it by an effective parameter. It will be shown below that α has the meaning of the internal friction coefficient assumed in the bulk material models.

Let $\alpha = 0$ in the case when complete adaptation of the elements to each other is possible. The value of α grows with the increase of a number of restrictions to the joint plastic deformation. That is, the less efficient are the mechanisms of plastic deformation of the structural elements, the higher is α.

The physical investigations show [10] that the growth of hydrostatic pressure gives rise to inclusion of new channels of plastic deformation. And there is a number of critical pressures which, being exceeded, activate new deformation mechanisms. Thus it follows that the value of α should decrease with the increase in pressure p. And it should be noted that at intermediate pressures (i.e. those between the critical ones) α does not depend on p. We show below that on the basis of this physical model the principal relationships can be derived which describe qualitatively the main peculiarities of the plastic deformation of compact, porous and powder materials under pressure.

3. PRINCIPAL RELATIONSHIPS OF THE MATHEMATICAL MODEL OF A SOLID BODY

The principal relationships of the flow theory have the form [13]

$$\dot{e}_{ij} = \lambda \frac{\partial f}{\partial \sigma_{ij}}; \tag{1}$$

here the following conditions are fulfilled:

$$\text{at } f = 0, \quad \frac{\mathrm{d}f}{\mathrm{d}t} = 0, \quad \frac{\partial f}{\partial \sigma_{ij}} \mathrm{d}\sigma_{ij} \neq 0 - \lambda > 0 \tag{2}$$

$$\text{at } f = 0, \quad \frac{\mathrm{d}f}{\mathrm{d}t} = 0, \quad \frac{\partial f}{\partial \sigma_{ij}} \mathrm{d}\sigma_{ij} = 0 - \lambda = 0 \tag{3}$$

$$\text{at } f = 0, \quad \frac{\mathrm{d}f}{\mathrm{d}t} < 0, \quad -\lambda = 0 \tag{4}$$

$$\text{at } f < 0, \quad -\lambda = 0. \tag{5}$$

where σ_{ij} and $\dot{e}_{ij}$ are the tensor components of stresses and rates of plastic deformation, respectively; f is the loading function; λ is the Lagrange factor.

Relationship (1) is the mathematical expression of the gradient condition.

Conditions (2)–(5) show that the plastic deformation takes place only when the stresses satisfy the condition of yielding

$$f = 0 \tag{6}$$

at the time moment under consideration and the closest one to it and the stress increment vector does not lie on the loading surface.

Condition (2) is assumed by us in an extended form to take into account the possible loss of the material stability stated in Section 1 (for stable materials in condition (2) $(\partial f/\partial \sigma_{ik})\mathrm{d}\sigma_{ik} > 0$, [13]).

The expression for loading function f should be chosen so as to make relationships (1) reflect the experimentally observed effects. It can be constructed on the basis of the proposed physical model of a solid body.

It was stated above that the proposed material differs from the conventional porous ones by the fact that its carcass has its own structure and it can get loosened at the deformation like bulk medium does.

It was shown [14, 15] that of all the known loading functions of isotropic porous bodies the best agreement with experiment is given by

$$f_1 = \frac{\sigma^2}{\psi(\theta)} + \frac{\tau^2}{\varphi(\theta)} - (1-\theta)k^2, \tag{7}$$

where $\sigma = \frac{1}{3}\sigma_{ik}\delta_{ik}$ is the hydrostatic component of the stress tensor; $\tau = \sqrt{((\sigma_{ik} - \frac{1}{3}\sigma\delta_{ik})(\sigma_{ik} - \frac{1}{3}\sigma\delta_{ik}))}$ is the stress deviator intensity; θ is the relative porosity; and k is the stress deviator intensity in the porous body carcass.

Porosity functions $\varphi(\theta)$ and $\psi(\theta)$ are chosen so as to provide the limiting transition to the von Mises yielding condition for compact material. That is, $\lim_{\theta\to 0} \varphi = 1$, $\lim_{\theta\to 0} \psi = \infty$. Their explicit form is obtained both experimentally and theoretically. In the latter case the irreversible change in the porous body volume is assumed to be connected with the change in the size of separate spherical pores. It is shown [16] that

$$\psi(\theta) = \frac{2}{3}\frac{(1-\theta)^3}{\theta}, \quad \varphi(\theta) = (1-\theta)^2. \tag{8}$$

At the experimental determination $\psi(\theta)$ and $\varphi(\theta)$ are set by the structure of these functions whose parameters are obtained by the model calibration in the experiment.

The most common is the structure of the following form:

$$\psi = \frac{(1-\theta)^{2n-1}}{6a\theta^m}, \quad \varphi = (1-\theta)^{2n-1}, \tag{9}$$

where n, m and a are the parameters.

The experimental technique of determination of these parameters is given in ref. [17].

The value of k in eq. (7) characterizes the behaviour of the porous body carcass at plastic deformation. For the ideal plastic carcass

$$k = \sqrt{\tfrac{2}{3}}\sigma_y, \tag{10}$$

where σ_y is the carcass yield stress.

For the stress-hardened carcass

$$k = \sqrt{\tfrac{2}{3}}\sigma_s(\Gamma_0), \tag{11}$$

where σ_s is the deformation resistance of the carcass; Γ_0 is the accumulated plastic deformation of the carcass determined by the following formula [16]:

$$\Gamma_0 = \int_0^t \frac{1}{\sqrt{(1-\theta)}} \sqrt{(\psi\dot{e}^2 + \varphi\dot{\gamma}^2)}\, dt, \tag{12}$$

where $\dot{e} = \dot{e}_{ik}\delta_{ik}$ is the first invariant of the deformation rate tensor; $\gamma = \sqrt{((\dot{e}_{ik} - \frac{1}{3}\dot{e}\delta_{ik})(\dot{e}_{ik} - \frac{1}{3}\dot{e}\delta_{ik}))}$ is the intensity of the deformation rate deviator; t is the time or some other parameter substituting it.

We take into consideration the fact that the proposed material has a structurally nonuniform carcass which in the course of deformation acts as soil medium. So, let us represent k in the form following from the limiting equilibrium condition for this medium [7]:

$$f_2 = \tau - k_0 + \alpha\sigma = 0, \tag{13}$$

where f_2 is the loading function of soil medium; k_0 is the shear adhesion coefficient; α is the internal friction coefficient.

In accordance with the above stated physical meaning of k we have from eq. (13)

$$k = k_0 - \alpha\sigma; \tag{14}$$

substituting the latter relationship into (7) we obtain the expression for the loading function of the proposed material

$$f = \frac{\sigma^2}{\psi(\theta)} + \frac{t^2}{\varphi(\theta)} - (1-\theta)(k_0 - \alpha\sigma)^2. \tag{15}$$

Substituting eq. (13) as a loading function in eq. (1) we obtain

$$\dot{e} = \alpha\dot{\gamma}. \tag{16}$$

Hence it follows that the carcass of the proposed material gets loosened at shear strains. The physical causes of this were discussed above where they were connected with the presence of the inherent structure of the carcass and the impossibility of complete accommodation of different structural elements to each other. The comparison of relationship (16) with the analysis made in Section 2 shows that internal friction coefficient α can be chosen as a quantitative measure of restrictions on the joint plastic deformation of different structural elements (loosening intensity is proportional to α).

According to Section 2 the value of α should decrease with the growth of pressure p, as was mentioned above, α being independent of P in the intervals between the critical pressures. When the maximum critical pressure is exceeded, i.e. when the acting deformation mechanisms provide complete accommodation of the structural elements to each other, $\alpha = 0$.

According to relationships (1) and (2) the following group of physical equations is connected with loading function (15):

$$\frac{\sigma^2}{\psi(\theta)} + \frac{\tau^2}{\varphi(\theta)} = (1-\theta)(k_0 - \alpha\sigma)^2 \tag{17}$$

$$\frac{\dot{e}\tau}{\varphi(\theta)} = \dot{\gamma}\left(\frac{\sigma}{\psi(\theta)} + \alpha(1-\theta)(k_0 - \alpha\sigma)\right) \tag{18}$$

$$\dot{e}_{ij} - \tfrac{1}{3}\dot{e}\delta_{ij} = \frac{\dot{\gamma}}{\tau}(\sigma_{ij} - \sigma\delta_{ij}). \tag{19}$$

While deriving eqs (18) and (19) we assumed α and k to be independent of σ, i.e. we can state that these relationships are valid in the intervals between the critical pressures.

Let us investigate the behaviour of the model material at proportional loading. Assuming $\tau \neq 0$ we divide eqs (17) and (18) termwise τ and obtain

$$\frac{\eta^2}{\psi} + \frac{1}{\varphi} = (1-\theta)\left(\frac{k_0}{\tau} - \alpha\eta\right)^2 \tag{20}$$

$$\frac{\dot{e}}{\varphi} = \dot{\gamma}\left(\frac{\eta}{\psi} + \alpha(1-\theta)\left(\frac{k_0}{\tau} - \alpha\eta\right)\right), \tag{21}$$

where $\eta = \sigma/\tau$ is the rigidity index of the stressed state. At proportional loading $\eta = \text{const}$.

Equation (20) yields

$$\tilde{\tau} = \frac{\tau}{k_0} = \frac{1}{\alpha\eta + \dfrac{1}{\sqrt{(1-\theta)}}\sqrt{\left(\dfrac{\eta^2}{\psi} + \dfrac{1}{\varphi}\right)}}. \tag{22}$$

Hence the first qualitative conclusion can be drawn: at proportional loading of the porous body with the loosening carcass ($\alpha > 0$) at compressing loads ($\eta < 0$) the stress deviator intensity is higher than that of the conventional porous material ($\alpha = 0$); at tensile loads ($\eta > 0$) the relationship is inverse.

This conclusion has an apparent physical meaning if one bears in mind that at the deformation of the loosening material the external pressure performs negative work and counteracts the deformation.

Substituting eq. (22) into eq. (21), we obtain

$$\dot{e} = \dot{\gamma}\varphi\left(\frac{\eta}{\psi} + \alpha\sqrt{(1-\theta)}\sqrt{\left(\frac{1}{\varphi} + \frac{\eta^2}{\psi}\right)}\right). \tag{23}$$

Let us analyse this relationship. It includes two terms having different physical meanings.

The first term in brackets in eq. (23) is characteristic for the models of porous bodies with a structureless carcass (i.e. $\alpha = 0$). Physically it corresponds to the isotropic growth ($\dot{e} > 0$ at $\eta > 0$) and decrease ($\dot{e} < 0$ at $\eta < 0$) in the number of pores present in the material.

The second term in brackets in eq. (23) is always greater than 0 and it describes the appearance of inhomogeneities. Since at $\alpha = 0$ this term turns to zero, the physical cause of the appearance of inhomogeneities is the restriction on joint coordinated deformation of different structural elements.

At pressures exceeding the maximum critical one, $\alpha = 0$, and new inhomogeneities do not appear, which is in agreement with the results of the physical investigations.

Thus relationship (23) describes both appearance and healing of micropores at compressing loads (at $\eta < 0$).

Taking into account the relationship $\dot{e} = \dot{\theta}/(1-\theta)$, we obtain the following kinetic equation for porosity θ from eq. (23):

$$\frac{\mathrm{d}\theta}{\mathrm{d}\gamma} = \varphi(1-\theta)\left(\frac{\eta}{\psi} + \alpha\sqrt{(1-\theta)}\sqrt{\left(\frac{1}{\varphi} + \frac{\eta^2}{\psi}\right)}\right). \tag{24}$$

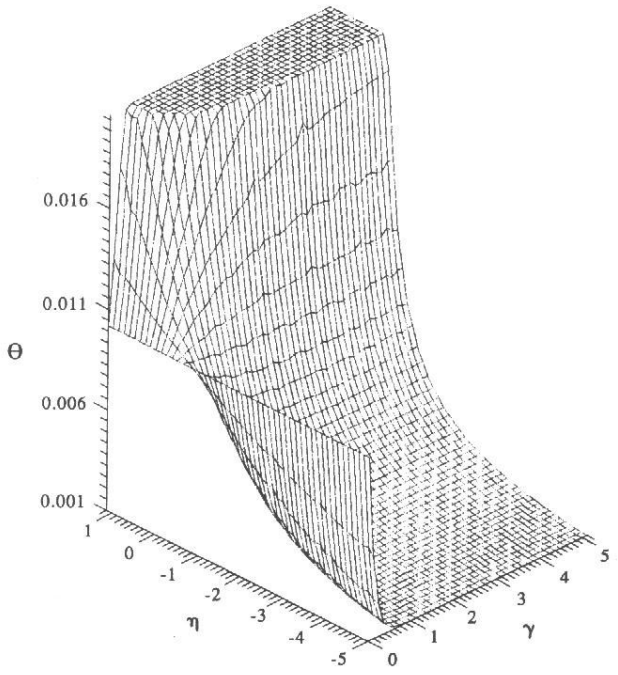

Fig. 1. The calculated dependence of porosity θ on the deformation value γ and stressed state rigidity index η (in the calculations: $\theta_0 = 0.01$; $\alpha = 0.01$).

From the latter equation the second qualitative conclusion can be drawn: at proportional loading, at $\eta < 0$, the material porosity tends asymptotically to the value of θ_p which is the root of the equation

$$\frac{\eta}{\psi(\theta_p)} + \alpha\sqrt{(1-\theta_p)}\sqrt{\left(\frac{1}{\varphi(\theta_p)} + \frac{\eta^2}{\psi(\theta_p)}\right)} = 0. \tag{25}$$

This conclusion corresponds to experiment [18].

Figure 1 illustrates the behaviour of the solution of eq. (24) by an example of dependence $\theta = \theta(\gamma, \eta)$. Functions φ and ψ are taken in the form of eq. (8), $\alpha = 0.001$, and the initial value of porosity $\theta_0 = 0.01$. It is seen clearly that in the dependence on η both loosening and compacting of the material is possible. And finally a certain, quite definite for the particular η, equilibrium porosity θ_p is set up.

4. SIMULATION OF VISCOUS FRACTURE UNDER PRESSURE

According to the present-day concepts (e.g. ref. [19]) the process of material fracture at plastic deformation is a multistage and multiscale one. It proceeds at various structural levels, the fracture at a lower level preparing the fracture at a higher level: the secondary defects are formed due to merging of the primary ones, the tertiary defects are formed due to merging of the secondary ones and so on. Up to some moment the defects of the same level are developed in a self-similar way, i.e. as the damage grows the geometry of the defect cascade is transformed in a similar way (the similarity principle [20]). The violation of the self-similarity is associated with the appearance of the defect of the next level [20].

Processes similar to the above one can be adequately investigated by means of percolation theory [21].

Let us give here some definitions and results of this theory which will be used in what follows for the construction of the model of the viscous fracture of the material at plastic deformation under pressure.

Let us assume that a big volume of space is chaotically filled with some substance. The volume fraction occupied by the substance is v. If $v \ll 1$ the substance forms small isolated regions. When

v increases the regions merge to form clusters. As v grows the cluster dimensions increase and at some critical value v_c a cluster occupying the entire volume is formed. This cluster is referred to as an infinite cluster. For volume tasks $v_c = 0.17$ (in a plane case $v_c = 0.50$).

The cluster contours are quite random. On the average, however, the geometry of chaotically located substance has quite definite properties when v approaches v_c. One of these properties is characterized by the similarity hypothesis which consists of the fact that when v approaches v_c the cluster geometry is transformed in a similar way, all linear dimensions increasing proportionally to the magnitude of $|v_c - v|^{-\nu}$. For the volume tasks $\nu = 0.9$ (in a plane case $\nu = 1.3$).

Let us assume that at each scale level there is a corresponding elementary defect, i.e. fracture atom. The cluster of fracture atoms forms the defect of this level. An infinite cluster of fracture atoms of the same level yields a fracture atom of the next level. Thus defects are brought in correspondence to clusters. Hence immediately follows the similarity principle for defects proved experimentally [20]. It consists of the fact that at multiple fracture the defect cascade is transformed in a similar way and all the linear dimensions of the cascade grow proportionally to the statistically average size of the defects.

In fact, the similarity principle is in this particular case the manifestation of regularities in the cluster development which are characterized by the percolation theory similarity hypothesis.

According to ref. [21] an infinite cluster is formed at a certain concentration of the cluster-forming matter (voids in our case) and is due to the loss of the self-similarity. This is also in agreement with experiment and explains the meaning of the concentration criterion of fracture (see ref. [1]).

According to ref. [1] the elementary act of fracture is the formation of microinhomogeneities with the linear dimension of 0.1 μm. The merging of these defects yields microinhomogeneities with the dimension of the order of the linear dimension of the structural heterogeneity (block, grain). The merging of the latter gives rise to the appearance of a macrocrack. Thus in terms of the model proposed we have: microinhomogeneity of 0.1 μm size, i.e. the fracture atom of the first level; microinhomogeneity with the size of structural heterogeneity, i.e. the fracture atom of the 2nd level; microcrack, i.e. the fracture atom of the 3rd level.

In accordance with the percolation theory, for an infinite cluster of some substance to be formed the relative fraction of this substance must achieve critical magnitude v_c.

Thus for the fracture atom of the 3rd level to be formed in unit volume of a body, v_c fracture atoms of the 2nd level and $v_c \times v_c$ fracture atoms of the 1st level are necessary. So, the critical magnitude of loosening is $\theta_c = v_c^2$. Substituting into this expression $v_c = 0.17$, we obtain $\theta \sim 3\%$, which is of the same order as the experimental value $\theta_c \sim 1\%$ [1].

In accordance with the similarity principle the cluster geometry of the defect cascade is determined by the defect relative volume, i.e. porosity.

On the basis of eq. (24) we obtain a kinetic equation for microporosity. For this purpose we assume $\varphi(\theta)$ and $\psi(\theta)$ in the form of eq. (9); suppose, according to ref. [22], that $m \approx 1$; take into account the fact that for compact materials $\theta \ll 1$ and $\alpha \ll 1$ and neglect the terms of the second order of smallness in eq. (24). Then we obtain

$$\frac{d\theta}{d\gamma} = \alpha + 6a\theta\eta. \tag{26}$$

The structure of kinetic equations (26) fully corresponds to the equation for the damage postulated in ref. [23]. The first term of eq. (26) describes the processes of appearance of microinhomogeneities whereas the second one represents their healing at $\eta < 0$.

We can show that eq. (26) and the concentration criterion of fracture can yield the expression for plasticity.

According to ref. [23] the term "plasticity" is understood as the value of shear deformation intensity Λ at the constant index of the stressed state rigidity σ/T (here T is the tangential stress intensity). Let us integrate eq. (26) with the initial condition $\gamma = 0$, $\theta = 0$ up to $\theta = \theta_c$ and obtain

$$\Lambda_p = \frac{1}{3a(\sigma/T)} \ln\left(1 + 3a(\sigma/T)\frac{\sqrt{2}\theta_c}{\alpha}\right), \tag{27}$$

where Λ_p is the ultimate plasticity.

In deriving relationship (27) we assumed that $\tau = T\sqrt{2}$ and $\gamma = (1/\sqrt{2})\Lambda$. Now let us analyse the obtained expression.

First of all it follows from eq. (27) that at $\sigma/T \to 0$, $\Lambda_p \to \sqrt{2}\theta_c/\alpha$. Thus we can right away obtain the expression for plasticity at torsion

$$\Lambda_p = \sqrt{2}\frac{\theta_c}{\alpha}. \tag{28}$$

Equation (27) also implies that $\Lambda_p \to \infty$ at

$$\sigma/T \to -\frac{\alpha}{3\sqrt{2}a\theta_c}. \tag{29}$$

This is the evidence of the fact that at rather large values of σ/T a state with infinite deformability is possible. This conclusion is in agreement with experiment [23]. The explanation of this phenomenon within the framework of the proposed fracture model consists of the fact that at rather large pressures the equilibrium value of porosity is lower than the critical one and the latter cannot be achieved.

Let us substitute eq. (28) into eq. (29) to obtain the expression for plasticity at compression (at $\sigma/T = -1/\sqrt{3}$) and tension (at $\sigma/T = 1/\sqrt{3}$):

$$\Lambda_{pc} = -\frac{1}{\sqrt{3}a}\ln(1 - \sqrt{3}a\Lambda_{pk})$$
$$\Lambda_{pp} = \frac{1}{\sqrt{3}a}\ln(1 + \sqrt{3}a\Lambda_{pk}). \tag{30}$$

It was shown [24] that the experimental values of Λ_{pk}, Λ_{pc} and Λ_{pp} for a lot of metals satisfy the approximate relationship

$$\Lambda_{pk} = \frac{2\Lambda_{pc}\Lambda_{pp}}{\Lambda_{pc} + \Lambda_{pp}}. \tag{31}$$

We show below that for metals $a \approx 0.05$–0.15. One can show that at these values of a and $\Lambda_{pk} \sim 1$ eqs (30) satisfy, with rather good accuracy, eq. (31). Figure 2 shows dependence of the right-hand side of eq. (31) on Λ_{pk} plotted in accordance with eqs (30) at $a = 0.1$ (the magnitudes of a within the range of $0.05 < a < 0.15$ produce almost no effect on the plot in Fig. 2). The plot also shows the experimental results given in ref. [24].

Figure 2 shows that the expression for plasticity (27) obtained on the basis of the proposed fracture model satisfies the experimentally observed connection between the values of plasticity at compression, torsion and tension. Thus if one determines parameter a by the results of uniaxial compression the experimental dependence

$$\Lambda_p = \frac{1}{3a(\sigma/T)}\ln[1 + 3(\sigma/T)\Lambda_{pk}] \tag{32}$$

automatically satisfies the uniaxial tension experiment. In view of the qualitative correspondence of the character of dependence (32) to the experiments [23] one can expect rather a good quantitative description of the experimental plasticity curves.

The above assumption is confirmed by Fig. 3, which gives theoretical and experimental plasticity curves for different metals. Parameter a of eq. (32) is determined by the experimental values of Λ_{pc}. Its magnitudes are given in Table 1, along with the magnitudes of α obtained on the basis of relationship (28) at $\theta_c = 0.01$.

These values of α and a will be used below for the theoretical prediction of the axial porosity of billets at hydroextrusion.

It was assumed above that the magnitude of α is not affected by the deformation. This assumption seems to be justified at the stage of simple (or close to simple) loading. At sharp bending in the deformation path, in the vicinity of the bending point there is unsteady deformation which is accompanied by blocking of microshifts and increase of internal microstresses. This process causes the strain-hardening of the material at small deformations. This process will obviously result in decreasing accommodation ability of structural elements, i.e. in higher α. Approximating

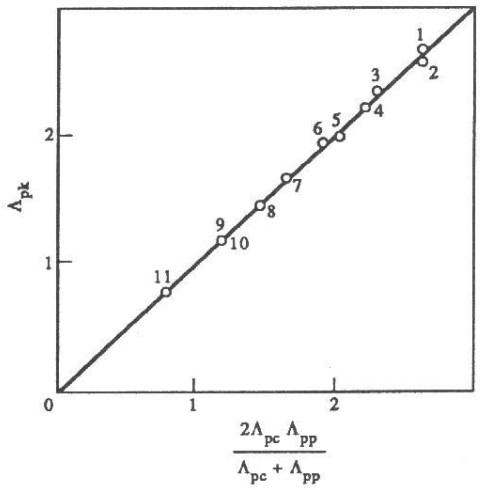

Fig. 2. Comparison of the experimental data ○ and the calculated dependence using eq. (31) (values in wt.%): 1—structural heat-resistant steel (0.11 C; 1.12 Cr; 0.55 Mn; 0.22 V; 0.35 Mo); 2—structural alloyed steel (0.19 C; 0.93 Cr; 0.65 Mn; 0.22 Si); 3—stainless steel (0.10 C; 17.7 Cr; 8.2 Ni; 0.74 Ti; 0.9 Mn; 0.6 Si); 4—structural carbon steel (0.21 C; 0.44 Mn; 0.18 Si); 5—titanium α—alloy (99.7 Ti); 6—structural carbon steel (0.24 C; 0.18 Si; 0.36 Mn); 7—structural alloyed steel (0.29 C; 0.93 Cr; 0.52 Mn; 0.27 Si; 0.22 Mo); 8—structural carbon steel (0.44 C; 0.48 Mn); 9—titanium pseudo-α-alloy (4.2 Al; 1.4 Mn); 10—structural carbon steel (0.47 C; 0.78 Mn); 11—titanium ($\alpha+\beta$)-alloy (5.4 Al; 3.1 Mo; 1.3 V).

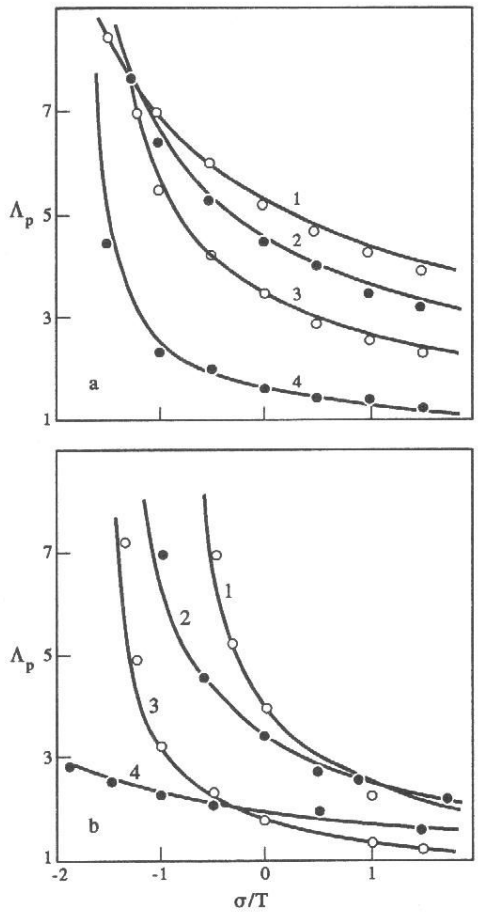

Fig. 3. Plasticity curves for different commercial materials (chemical composition in wt.%): (a) 1—armco Fe (99.98 Fe); 2—structural carbon steel C_T3 (0.16 C; 0.38 Mn); 3—structural carbon steel 45 (0.46 C; 0.52 Mn; 0.18 Si); 4—structural ball-bearing steel III × 15 (0.98 C; 1.43 Cr; 0.28 Mn; 0.22 Si); (b) 1—deformable aluminium alloy AII-1 (99.5 Al); 2—structural alloyed steel 40X (0.37 C; 0.88 Cr; 0.64 Mn; 0.24 Si); 3—structural alloyed steel 30XГCA (0.31 C; 0.95 Cr; 1.06 Mn; 0.94 Si); 4—stainless steel X18H1OT (0.06 C; 17.8 Cr; 9.9 Ni; 0.7 Ti; 1.2 Mn). ○ and ● denote experiment (Table 1); ——denotes calculation (the values of α and a are given in Table 1).

Table 1. Values of the model parameters determined by the material plasticity at torsion and compression

No.	Material	Λ_{pk}	Λ_{pc}	Source	$a \times 10^2$	$\alpha \times 10^3$
1	α-Fe	5.3	6.1	†	2.7	2.7
2	S C_T3	4.6	5.5	†	3.9	2.6
3	t 45	3.5	4.4	†	6.3	4.0
4	e 40X	3.4	4.5	†	7.6	4.2
5	e III × 15	1.6	2.0	[23]	13.4	8.9
6	l 30XГCA	1.8	2.3	[23]	12.9	7.9
7	s X18H10T	1.9	2.1	[23]	5.6	7.5
8	Alloy AII – 1	4.0	8.0	[23]	11.5	3.5

†The data are given to us by the courtesy of V. S. Smirnov.

dependence of α on γ by the power function (as is done at the approximation of the hardening curves at small deformations), we obtain

$$\alpha = \alpha_0 \gamma^n. \tag{33}$$

Substituting eq. (33) into kinetic eq. (26) and neglecting the term due to the defect healing, we obtain

$$\frac{d\theta}{d\gamma} = \alpha_0 \gamma^n. \tag{34}$$

The form of this kinetic equation coincides with the equation for the damage suggested in ref. [24] for description of the processes with sharp bends in the deformation path.

5. STABILITY AND LOCALIZATION OF PLASTIC DEFORMATION UNDER PRESSURE

The common feature for all plastic bodies is the fact that when a certain critical value ϵ_{cr} is achieved the deformation is rather smooth and the continuous picture of plastic yield is replaced by highly localized deformation in the form of shear bands. This phenomenon is referred to as the loss of stability of the "material" type.

Sometimes the shear bands, once formed, persist and the following deformation proceeds in a substantially nonuniform way. More often, however, the localization of deformation produces viscous fracture and the loss of the deformation stability can be regarded as a fracture criterion.

One of the physical causes of the deformation stability loss is weakening of the material due to its loosening.

The proposed model material can become loosened at deformation and therefore be used for the investigation of the stability loss due to the above cause.

According to ref. [25] the stable deformation condition has the form

$$\frac{\partial f}{\partial \sigma} d\sigma + \frac{\partial f}{\partial \tau} d\tau > 0. \tag{35}$$

It should be taken into consideration that $f = f(\sigma, \tau, \theta, \Gamma_0)$ and at plastic deformation $df = 0$, i.e.

$$\frac{\partial f}{\partial \sigma} d\sigma + \frac{\partial f}{\partial \tau} d\tau + \frac{\partial f}{\partial \theta} d\theta + \frac{\partial f}{\partial \Gamma_0} d\Gamma_0 = 0. \tag{36}$$

From eqs (35) and (36), we obtain an equivalent stability condition

$$\frac{\partial f}{\partial \theta} d\theta + \frac{\partial f}{\partial \Gamma_0} d\Gamma_0 < 0. \tag{37}$$

The latter relationship shows that the deformation of the material with the non-hardening carcass is stable only at its compaction. In fact, setting $\partial f / \partial \Gamma_0 = 0$ we obtain from eq. (37)

$$\frac{\partial f}{\partial \theta} d\theta < 0.$$

It follows from eqs (15) and (9) that $\partial f / \partial \theta > 0$. Therefore, the stability condition in this case has the form $d\theta < 0$, i.e. the material is stable only at compaction. The loosening of the material with the non-hardening carcass is associated with the deformation localization.

Let us investigate the pressure effect on the stability of the model material. Assuming the pressure value to be constant we obtain the following stability condition from eq. (35):

$$\frac{\partial f}{\partial \tau} d\tau > 0. \tag{38}$$

Since $\partial f / \partial \tau > 0$, eq. (38) yields the stability condition in the form of

$$d\tau > 0. \tag{39}$$

Thus the deformation process is stable if in its course the magnitude of the stress deviator intensity increases. This conclusion is independent of whether the material carcass gets hardened or not.

We obtain the system of equations describing the deformation of the model material at the constant pressure and investigate the stability of the solution of this system according to criterion (39). Here we shall not restrict ourselves to the condition $\theta \ll 1$. From eq. (17) it follows that

$$\tau = \sqrt{(\varphi^{(\theta)})}\sqrt{\left((1-\theta)(k_0-\alpha\sigma)^2 - \frac{\sigma^2}{\psi(\theta)}\right)}. \tag{40}$$

Substituting this expression into eq. (18) and taking into consideration the connection betwen $\dot{e}$ and $\dot{\theta}$, we obtain the kinetic equation for porosity

$$\frac{\mathrm{d}\theta}{\mathrm{d}\gamma}\tau(\theta) = (1-\theta)\varphi(\theta)\left(\frac{\sigma}{\psi(\theta)} + \alpha(1-\theta)(k_0-\alpha\sigma)\right), \tag{41}$$

where $\tau(\theta)$ is determined by relationship (40).

In numerical integration of eq. (41) we took into consideration the possibility of strain-hardening of the carcass by the power law:

$$k_0 = C_1 + C_2 \times \Gamma_0^n.$$

For this purpose the entire range of integration over γ was divided into N sections. Within each ith section k_0 was represented by its value at deformation, Γ_{0i}, determined for the beginning of the section. The value of N was chosen so as to provide the difference in the calculations at the number of divisions N and $N+1$ only in the fourth significant digit.

Figure 4 presents the plot of dependence $\bar{\tau} = \bar{\tau}(\gamma)$, where $\bar{\tau} = \tau/C_1$ at different levels of hydrostatic pressure. We assumed in the calculations that $C_1 = 1.0$, $C_2 = 0.2$, $n = 0.20$, $a = 0.10$, and $\alpha = 5 \times 10^{-3}$. From Fig. 4 and stability criterion (39) it follows that hydrostatic pressure growth increases the deformation stability of the model material.

6. CONCLUSION

The pressure effect on plasticity and stability of the "material" type can be described on the basis of the gradient condition and the loading function corresponding to the following physical model of the material.

—the representative volume of the material consists of a large number of interconnected structural elements which, in the course of deformation, can shift and rotate with respect to each other, split and deform plastically, thus adapting to each other;

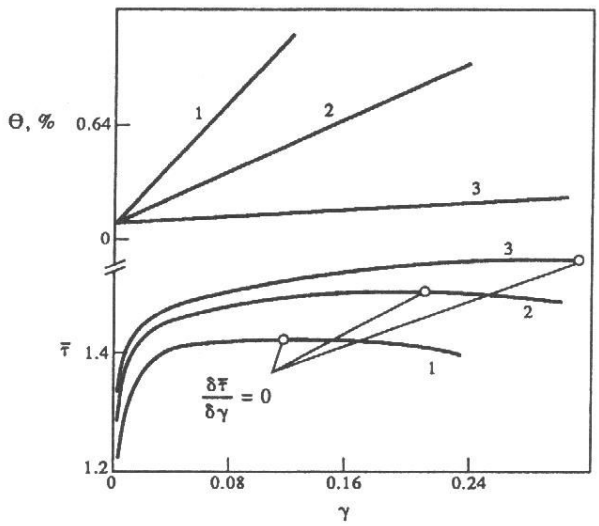

Fig. 4. The calculated dependencies of porosity θ and reduced intensity of stress deviator τ on deformation magnitude γ illustrating an increase in the "material"-type stability under pressure (in calculations: $C = 1.0$; $C_2 = 0.2$; $n = 0.20$; $a = 0.10$; $\alpha = 5 \times 10^{-3}$); 1—$\sigma/C_1 = 2$; 2—$\sigma/C_1 = 0$; 3—$\sigma/C_1 = -2$.

—at coordinated deformation of the structural elements, in the general case only partial adaptation is possible due to the presence of microinhomogeneities between them;

—adaptability is determined by the efficiency of the acting deformation mechanisms;

—restrictions on the coordinated deformation of the structural elements are characterized quantitatively by the magnitude of parameter α (internal friction coefficient); if complete adaptation is possible, $\alpha = 0$; otherwise $\alpha > 0$ and this parameter grows with the increase of a number of restrictions on the deformation of the structural elements;

—there is a number of critical pressures such that in the intervals between them α is independent of pressure and passing through them it drops abruptly as the pressure increases; at pressures higher than the maximum critical value $\alpha = 0$.

This simple description of such a rather complicated many-level system as deformed materials seems to be possible due to the fact that at monotonous loading without sharp bends in the deformation paths the system becomes self-organized.

From the general concepts of synergetics it is known that in this case the number of degrees of freedom of the system becomes reduced to several order parameters. That is why the complicated system acquires rather a simple behaviour not typical of its subsystems.

In the investigation of viscous fracture under pressure the material porosity acted as an order parameter.

REFERENCES

[1] V. I. Betekhtin, V. I. Vladimirov, A. G. Kadomtsev and A. I. Petrov, Plastic deformation and fracture of crystalline bodies. Report I. Deformation and development of microcracks. *Problemy prochnosti* **7,** 38–45 (1979).
[2] B. I. Beresnev, E. D. Martynov, K. P. Rodionov, V. N. Ryabinin and L. D. Lifshits, *Plasticity and Strength of Solid Bodies at High Pressures*. Nauka, Moscow (1970).
[3] M. Brandes, Mechanical properties of materials under hydrostatic pressure, in *Mechanical Properties of Materials Under High Pressure* (Edited by H. LI. D. Pugh), Volume 1, pp. 19–80. Mir, Moscow (1973).
[4] H. LI. D. Pugh (Ed.) *Mechanical Properties of Materials Under High Pressure*, Volume 2. Mir, Moscow (1973).
[5] B. I. Beresnev, K. I. Ezerskii, E. V. Trushin and B. I. Kamenetskii, *High Pressures in Modern Technologies of Metal Forming*. Nauka, Moscow (1988).
[6] A. L. Gerson, Continuum theory of viscous fracture due to generation and growth of pores. Part I. Yield criterion and flow laws for porous plastic medium. *Theor. Background Engng Calculations* **99,** 1–16 (1977).
[7] V. V. Novozhilov, On plastic loosening. *Prikl. mat. mekh.* **29,** 681–689 (1965).
[8] V. Tvergaard, Effect of yield surface curvature and void nucleation of plastic flow localization. *J. Mech. Phys. Solids* **35,** 43–91 (1987).
[9] A. Needleman and V. Tvergaard, A numerical study of void distribution effects on dynamic ductile crack growth. *Engng Fracture Mech.* **38,** 151–173 (1991).
[10] V. A. Streltsov, G. Ya. Akimov and I. Yu Prokhorov, Fracture of crystalline solids under hydrostatic pressure. *Fiz. tekh. vysokikh davlenii* **12,** 60–87 (1983).
[11] A. N. Mokhel, R. L. Salganik and S. A. Khristianovich, On plastic deformation of hardening metals and alloys. Principal equations and related calculations. *Mekh. tverdogo tela* **4,** 119–141 (1983).
[12] M. Oyane, S. Shima and Y. Kono, Theory of plasticity for porous metals. *Bull. JSME* **16,** 1254–1262 (1973).
[13] D. D. Ivlev and G. I. Bykovtsev, *Theory of Hardening Plastic Body*. Nauka, Moscow (1971).
[14] A. M. Laptev, Plasticity criteria of porous metals. *Poroshkovaya metall.* **7,** 12–18 (1982).
[15] V. Z. Midukov and V. D. Rud, The state of art in the experimental research of plastic deformations of porous materials, in *Rheological Models and Deformation Processes of Porous Powder and Composite Materials* (Edited by V. V. Skorokhod), pp. 61–67. Naukova Dumka, Kiev (1985).
[16] M. B. Shtern, G. G. Serdyuk, L. A. Maksimenko, U. V. Trukhan and U. M. Shuliakov, *Phenomenological Theories of Powder Compacting*. Naukova Dumka, Kiev (1982).
[17] L. N. Sokolov, A. M. Laptev and V. L. Malyuskii, Plasticity theory of porous bodies and its application for the calculation of hydrostatic treatment of powdered and sintered materials. *Fiz. tekh. vysokikh davlenii.* **11,** 38–41 (1993).
[18] A. W. Bishop, Shear strength parameters for undisturbed and remoulded soil specimens, in *Proceedings of the Rosccoe Memorial Symposium*, Cambridge University (Edited by R. H. G. Parry), pp. 3–58 (1972).
[19] V. I. Vladimirov, *Physical Nature of Metal Fracture. Metallurgija, Moscow* (1984).
[20] G. I. Barenblatt and L. R. Botvina, Similarity technique in the fracture mechanics. *Fiziki-khimicheskaja mekh. mater.* **22,** 57–62 (1986).
[21] B. I. Shklovskii and A. L. Efros, *Electronic Properties of Alloyed Semiconductors*. Nauka, Moscow (1979).
[22] A. M. Dmitriev and A. G. Ovchinnikov (Eds), *Progressive Technological Processes of Stamping Powder Materials and Equipment*. Mashinostrojenije, Moscow (1991).
[23] V. L. Kolmogorov, *Stresses, Deformations, Fracture. Metallurgija, Moscow* (1970).
[24] E. M. Makushok, A. V. Belyi, D. I. Dmitrovich and T. V. Kalinovskaya, *Engineering Theory of Plasticity*. Nauka i tekhnika, Minsk (1985).
[25] D. Drukker, On the postulate of material stability in the continuum mechanics. *Mekhanika* (collection of translations), **3**(85), 115–128 (1964).

(*Received* 28 *June* 1993)